J. Electr. Electron. Mater.
Vol. 38, No. 6, pp. 604-616 November 2025
doi: https://doi.org/10.4313/JEEM.2025.38.6.2
ISSN 1226-7945(Print), 2288-3258(Online)

Academic Progress Report

Recent Advances in Transfer and Bonding of Micro-LEDs for Micro-LED Display Fabrication

Jungho Shin and Jiho Joo

Creative & Basic Technology Research Division, Electronics and Telecommunications, Daejeon 34129, Korea

(Received August 25, 2025; Revised September 9, 2025; Accepted September 24, 2025)

Abstract: Micro-LEDs, which have a chip size of less than 100 × 100 μm², have been potential candidates for conventional LCDs and OLEDs due to their high optical power, outstanding stability, and nanosecond response time. However, Micro-LED chips are fabricated only on limited substrates due to the high-temperature metal–organic chemical vapor deposition process and lattice-mismatch issues. Therefore, the fabrication of Micro-LED displays requires complex processes such as chip fabrication, transfer, bonding, and repair. Especially, Micro-LED transfer and bonding have been critical challenges for the Micro-LED display commercialization. Here, recent advances in the transfer and bonding of Micro-LEDs are introduced, and novel Micro-LED display fabrication methods are reviewed to provide a practical outlook for both mass production and commercialization of Micro-LED displays.

Keywords: Micro-LED, Display, Transfer, Bonding

1. INTRODUCTION

Micro light-emitting diode (Micro-LED) displays have attracted great industrial attention to replace traditional liquid crystal displays and organic light-emitting diodes owing to their high optical performance, long device lifetime, and fast response time (~ ns) [1]. Since Apple acquired a Micro-LED startup called LuxVue in 2014, Micro-LED displays have been consistently developed and utilized in TVs, smartwatches, head-up displays, and AR/VR systems. Samsung and AUO introduced Micro-LED prototypes at global exhibitions including Consumer Electronics Show and SID display week. Especially, Micro-LED-based TVs are demonstrated at a large scale by seamlessly tiling small Micro-LED modules [2]. However, Micro-LED displays in these products have a critical challenge of low manufacturing yield, which hinders their commercialization [3]. To fabricate Micro-LED displays, epi-layers should be firstly grown on mother substrates including GaAs, sapphire, and Si. Unlike OLEDs, these epi-layers cannot be directly grown on display backplanes due to lattice mismatch issues and high-temperature (over 700°C) metal-organic chemical vapor deposition process [4,5]. Therefore, Micro-LED chips are generally fabricated on their own epi-wafers, and temporarily placed on donor substrates after laser lift-off. These LED chips are transferred from donor substrates to target substrates including backplanes or printed circuit boards (PCBs) via transfer heads, as schematically illustrated in Fig. 1(a). To transfer these micro-scale LEDs in both high precision and yield, many researchers have utilized various physical effects such as photothermal reactions [6], fluidic forces [7], electrostatic forces [8], electromagnetic forces [9], and Van del Waals interactions [10].

After the Micro-LED transfer, the micro-scale chips should be electrically connected to underlying substrates to display images, as described in Fig. 1(b). Between the Micro-LEDs and the electrodes of backplanes or PCBs, conductive

✉ **Jungho Shin; sjh0759@etri.re.kr**

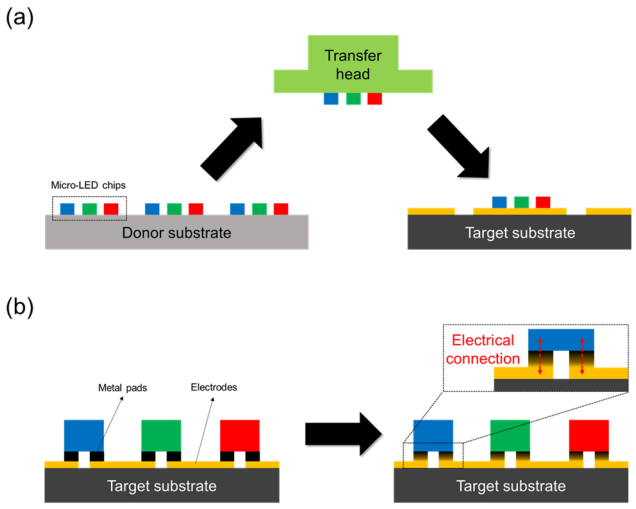

Fig. 1. (a) Schematic illustrations of Micro-LED transfer and (b) bonding for Micro-LED display fabrication.

materials such as metal-coated polymer balls, solders, and eutectic metals have been introduced, which deform under pressure and heat [11-13].

Herein, we introduce the overview of transfer and bonding techniques for Micro-LED display fabrication. Recent advances in the field of Micro-LED display manufacturing can be classified into three categories: (i) Micro-LED transfer methods, (ii) Micro-LED bonding techniques, and (iii) other novel Micro-LED display fabrication approaches. These perspectives will provide an outlook for identifying the current issues related to the commercialization of Micro-LED displays and devise future solutions.

2. MICRO-LED TRANSFER

2.1 Elastomer Stamping and Roll Transfer

Since Meitl et al. introduced the transfer printing of silicon microstructures and photodiodes onto soft substrates using polydimethylsiloxane (PDMS) stamp in 2006, elastomer stamping has been applied to transfer inorganic devices from rigid substrates to soft polymer substrates to fabricate flexible electronic devices [Fig. 2(a)] [10,14]. After uniform contact between the stamp and the devices, the adhesive stamp was rapidly peeled off to pick up the devices from their mother substrates. To release these inorganic devices onto target substrates, the stamp was slowly detached from target substrates. By exploiting these kinetic adhesion controls, many researchers have transferred the Micro-LEDs from mother substrates to flexible substrates, backplanes, and PCBs [15-17]. For instance, Park et al. demonstrated flexible red Micro-LEDs by transferring AlGaInP Micro-LED chips from GaAs substrates to polymeric substrates [Fig. 2(b)] [18]. The LED chips became free-standing with anchors by etching sacrificial layer between the LED epitaxy and GaAs substrates with concentrated hydrofluoric acid. Using a soft elastomeric stamp, 1,600 AlGaInP Micro-LEDs were picked up from the substrates, and released onto polyethylene terephthalate (PET) with a pitch of 1.4 mm, as shown in [Fig. 2(c)]. In order to exploit this elastomer stamping for mass production of Micro-LED displays, X-Display introduced an elastomer stamp consisting of 750 × 750 array of PDMS posts to selectively pick up Micro-LEDs from their mother substrates or donor substrates, and developed corresponding mass-transfer equipment [19]. Although elastomer stamping has been widely utilized for Micro-LED transfer, it has limitations such as susceptibility to contamination and limited recyclability. Roll-transfer utilizes the roll-based elastomer stamp to transfer Micro-LEDs onto target substrates in both high productivity and large-area scalability. By using the same transfer method, a 5.1-inch full-color Micro-LED display with a resolution of 320 × 160 was demonstrated. The yields of red, green, and blue subpixels were 100%, 99.996%, and 99.998%, respectively.

Choi et al. reported the roll-transfer for the heterogeneous integration of Micro-LEDs and Si thin-film transistors (TFTs) on polymer substrates, as schematically illustrated [Fig. 2(d)] [20]. Both Si-TFTs and AlGaInP Micro-LEDs were transferred from their mother substrates to carrier substrates through the roll-transfer process. The transfer yield of both devices was closed to 99.9% after optimizing the adhesion property of a roller and target substrates. By applying an additional roll-transfer, these inorganic devices were assembled on elastomer substrates, and integrated into a stretchable display. During the multiple roll-transfer process, these devices were precisely transferred without significant performance degradation, demonstrating the active-matrix stretchable Micro-LED display [Fig. 2(e)]. By the scalable roll-transfer process, blue Micro-LED chips were assembled on a meta-PCB to demonstrate a Micro-LED-based stretchable

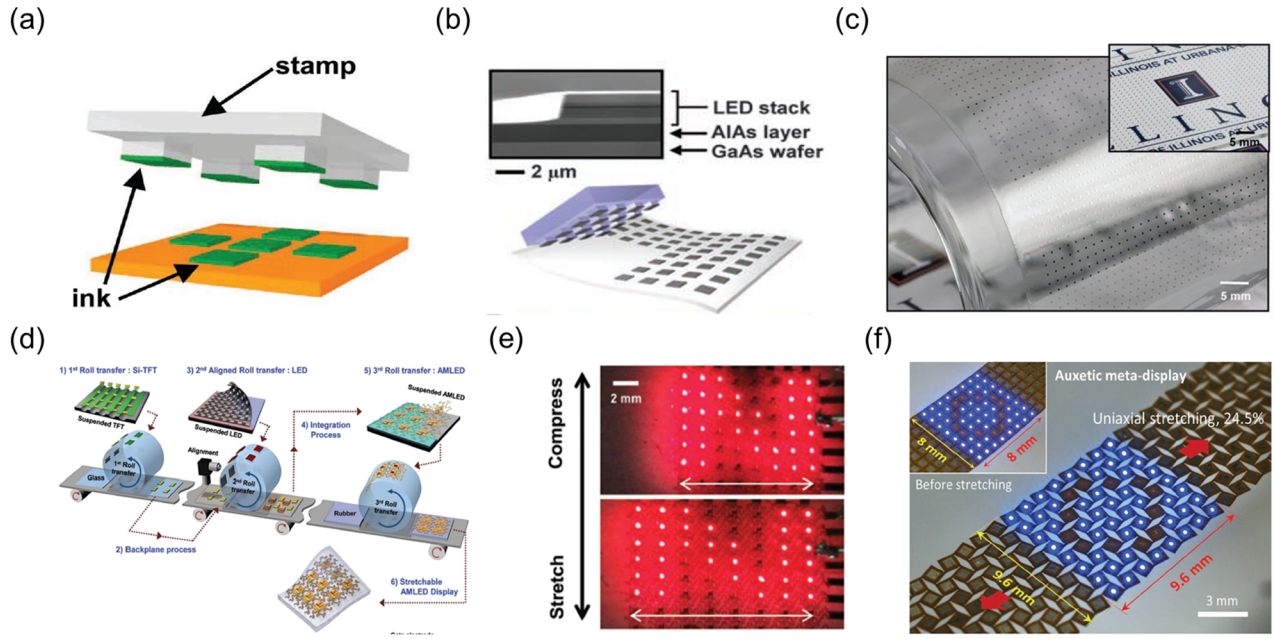

Fig. 2. (a) Schematic illustration of elastomer stamping (Reprinted with permission from ref. [14]. Copyright 2012, Wiley-VCH), (b) cross-sectional SEM image of AlGaInP Micro-LEDs on GaAs substrates and schematics of transferring these Micro-LEDs via elastomer stamping method, (c) photograph of 1,600 AlGaInP Micro-LEDs transferred on PET substrates with a pitch of 1.4 mm (Reprinted with permission from ref. [18] Copyright 2009, AAAS), (d) schematic illustration of roll-transfer method for the integration of Micro-LEDs and Si TFTs on polymer substrates, (e) photograph of a stretchable active-matrix Micro-LED display (Reprinted with permission from ref. [20]. Copyright 2017, Wiley-VCH), and (f) photograph of a Micro-LED-based stretchable meta-display fabricated by roll-transfer method (Reprinted with permission from ref. [21]. Copyright 2022, Wiley-VCH).

meta-display, as shown in Fig. 2(f) [21]. In this case, the flexible substrates incorporated kirigami cutting patterns and exhibited auxetic behavior with a Poisson's ratio of -1. Therefore, the Micro-LED display was stretched up to 22.6% strain, and conformally wrapped around a spherical surface without any serious crumpling.

2.2 Fluidic Self-Assembly

Fluidic self-assembly has also been applied to Micro-LED mass transfer. The Micro-LEDs dispersed in liquid solutions can be spontaneously placed on bonding pads of target substrates or transfer molds. To guide the free-standing chips to the specific locations, various physical forces such as electric forces [22], surface tensions [23], and magnetic forces [7] have been utilized. Chang et al. introduced the magnetic force-based fluidic self-assembly of Micro-LEDs to realize Micro-LED displays [7]. Magnetic rod arrays under target substrates moved in both x and y directions with rotational motion to cluster the free-standing Micro-LED chips and guide them to the holes of the substrates. Dielectrophoresis forces were also utilized for self-alignment of Micro-LED chips in the holes. By combining these forces, totally 43,200 Micro-LEDs were transferred onto the backplane to demonstrate a 120 × 120 resolution full-color Micro-LED display with the pixel yield of 99.98%.

In order to increase the yield of the fluidic self-assembly, the driving force of Micro-LED chips to be delivered to bonding pads of target substrates should be improved. For instance, the increase in the viscosity of liquid leads to high-yield Micro-LED transfer [23]. For LED chips smaller than 30 μm, the transfer yield onto the molten solders of target substrates was below 5% when the assembly solution had low viscosity. However, by increasing the liquid viscosity through the poloxamer addition, the transfer yield was improved to as high as 99%. In other way, the electric field was utilized to guide the chips onto the targeted regions of target substrates, which was even compatible to nanometer-scale LEDs [24]. Park et al. reported the assembly of green InGaN/GaN nanorod LEDs on Si substrates via fluidic self-assembly under electric

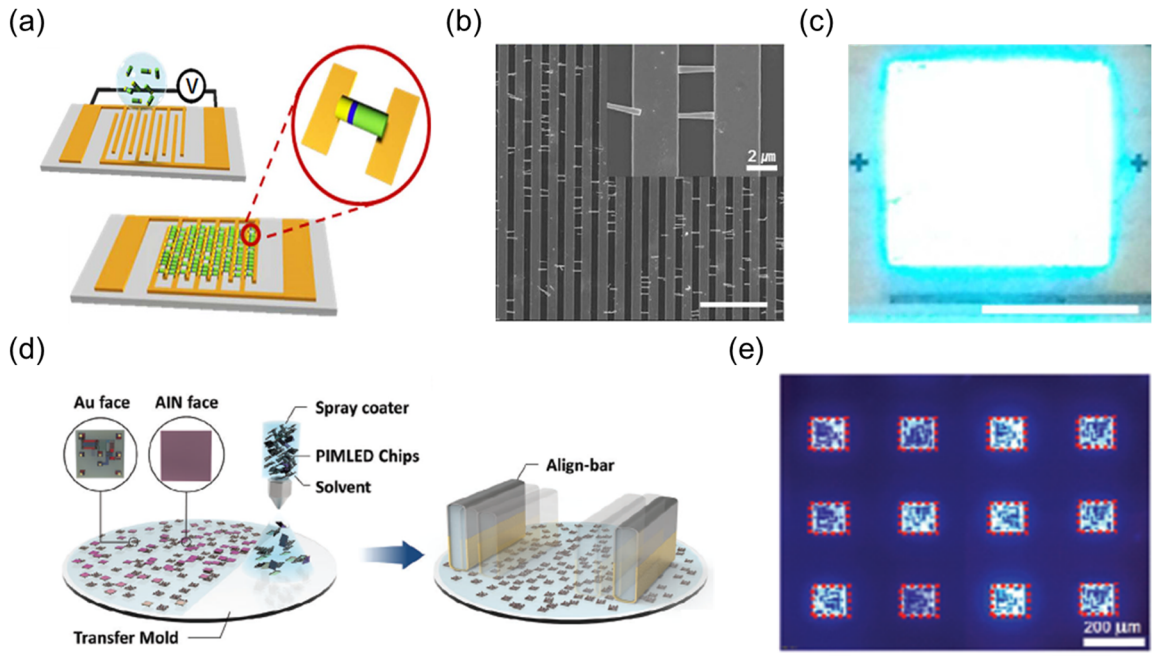

Fig. 3. (a) Schematic illustration of fluidic self-assembly of InGaN/GaN nanorod LEDs under electric field, (b) top-view SEM image of nanorod LEDs aligned with the interdigitated electrodes during the fluidic self-assembly, (c) electroluminescence of nanorod LEDs transferred by the fluidic self-assembly under electric field (Reprinted with permission from ref. [22]. Copyright 2016, Nature Publishing Group), (d) schematic illustration of misalignment-free transfer of pixel-circuit integrated Micro-LEDs, and (e) photoluminescence of pixel-circuit integrated Micro-LEDs transferred on the transfer mold (Reprinted with permission from ref. [25]. Copyright 2025, Wiley-VCH).

field [Fig. 3(a)] [22]. The nanorod LEDs were fabricated on sapphire substrates using a Cl_2-based reactive ion etching process, and suspended in acetone. After dispensing these green LEDs on Si substrates with Ti/Au electrodes, the nanorods were spontaneously aligned on the interdigitated electrodes, and formed electrical contact with them under bias, as shown in Fig. 3(b). Although the nanorod LEDs exhibited electroluminescence behavior after the transfer process, the operating voltage of transferred devices was too high for practical use in Micro-LED display [Fig. 3(c)]. However, note that electric field could be a powerful solution to drive the Micro-LED alignment on dense electrodes with widths of ~3 μm and spacings of ~2.5 μm.

Figure 3(d) presents the misalignment-free transfer of pixel-circuit integrated Micro-LEDs via fluidic self-assembly [25]. Both Micro-LED chips and low-temperature poly-silicon transistors were fabricated on GaN-on-Si wafer, followed by separating devices from Si substrates via KOH etching. Subsequently, the Micro-LEDs integrated with transistors were suspended in deionized water, and dispersed in transfer mold that had an array of holes to passively align the devices during the fluidic self-assembly. During the transfer process, an alignment bar was swept on the mold until all the devices were placed in the holes. The pixel-circuit integrated LED devices were passively aligned to the holes of the transfer mold, and exhibited stable photoluminescence, as shown in Fig. 3(e). To prevent the angular misalignment between the transferred Micro-LEDs and the backplanes, the electrodes of Micro-LEDs were designed with concentric circular patterns. These results indicate that the fluidic self-assembly enables the cost-effective transfer of Micro-LEDs without the use of sophisticated alignment equipment. The yield of this transfer method was measured to be in the range of 99.5 ~ 99.7% during the assembly of 9,216 Micro-LED chips. However, both production rate and yield of fluidic self-assembly remain below commercialization levels.

2.3 Other Micro-LED Transfer Methods

In addition to elastomer stamping, roll-transfer, and fluidic self-assembly, various Micro-LED transfer techniques have been introduced. For instance, some researchers proposed

electrostatic or electromagnetic transfer of Micro-LEDs, as schematically illustrated in Fig. 4(a) [26]. In both cases, the transfer head had the capability of generating electric field or magnetic field in specific regions, forming the attractive force with the Micro-LEDs attached to the carrier substrates. However, the Micro-LEDs can be seriously damaged during the transfer process due to the high voltage or magnetomotive force. Figure 4(b) shows the blister actuated laser-induced forward transfer of Micro-LEDs [27]. After picking up the Micro-LEDs from the mother substrates to the carrier substrates, the Micro-LEDs are selectively detached from the carrier substrates, and released onto the target substrates due to the laser irradiation. To decrease the adhesion between the Micro-LEDs and the carrier substrates, the laser was focused on the interface between the polyimide and the glass in the carrier substrates, resulting in the blister formation due to the photothermal decomposition of polyimide. Owing to this blister actuation, the contact area between the polyimide and the Micro-LEDs was significantly decreased, inducing the spontaneous release of devices on target substrates. In other cases, the laser was directly irradiated onto the adhesive material of carrier substrates to change its adhesion properties. The average transfer yield was 99.61% during 10 cycles of Micro-LED transfer. The laser-induced forward transfer has an advantage of selective transfer in a chip-level, however, exhibits the unintentional misalignment between the Micro-LEDs and the target substrates. Park et al. reported the Micro-LED transfer via the vacuum forces, as shown in Fig. 4(c) [28]. The vacuum controllable transfer module had two micro-channels, and hole arrays were connected to each channel. After the conformal contact between Micro-LEDs and holes, the external vacuum force applied suction to LEDs via the micro-channels and the holes in the transfer module. Due to this vacuum force, the micro-scale chips were picked up from their mother substrates. By the way, this suction force was immediately removed to transfer the Micro-LEDs from the transfer module to target substrates. Utilizing this vacuum-based transfer printing, the AlGaInP LEDs were transferred on the polyimide substrates to demonstrate the flexible Micro-LED device, as displayed in Fig. 4(d). The average transfer

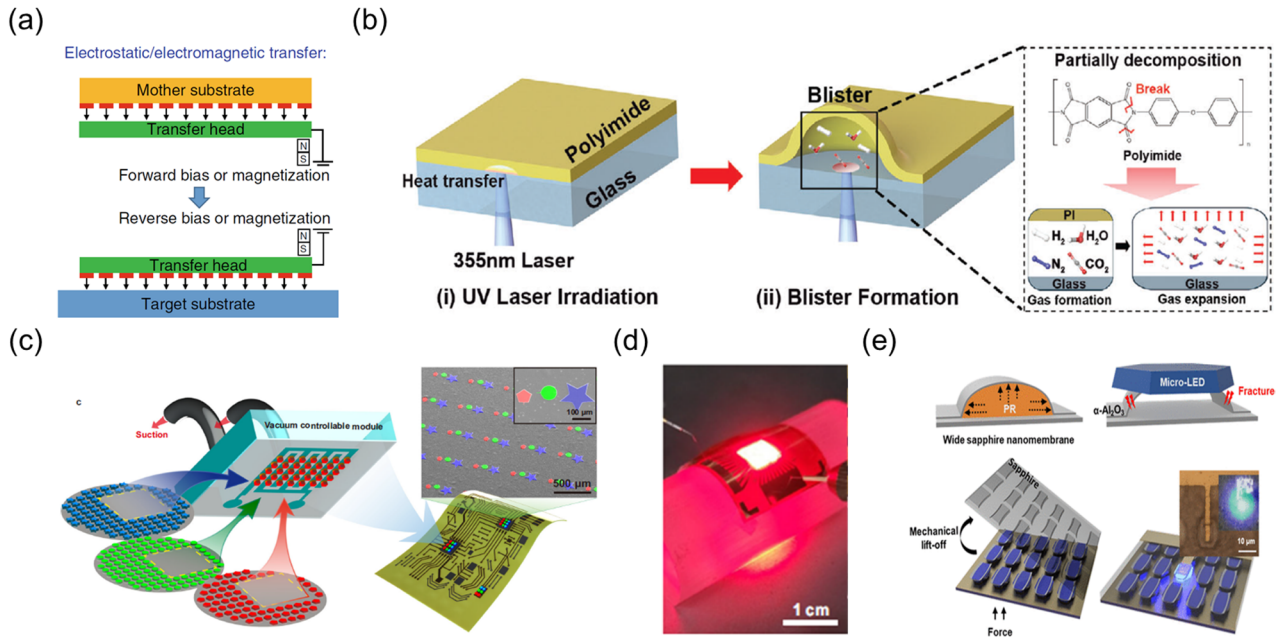

Fig. 4. (a) Schematic illustration of electrostatic/electromagnetic transfer (Reprinted with permission from ref. [26]. Copyright 2020, Nature Publishing Group), (b) schematic illustration of blister actuated laser-induced forward transfer that utilizes blister (Reprinted with permission from ref. [27]. Copyright 2024, Wiley-VCH), (c) schematic illustration of vacuum assisted Micro-LED transfer, (d) photograph of AlGaInP Micro-LEDs transferred on the polyimide substrates after the vacuum assisted transfer printing (Reprinted with permission from ref. [28]. Copyright 2023, Nature Publishing Group), and (e) schematic illustration of Al_2O_3 nanomembrane and its application for Micro-LED transfer (Reprinted with permission from ref. [29]. Copyright 2024, American Chemical Society).

yield was measured to be 98.06% during 100 cycles of transferring 10 × 10 Micro-LED arrays onto the target substrates. Note that the Micro-LEDs exhibited consistent photoluminescence and I-V characteristic regardless of vacuum-based Micro-LED transfer. This transfer method enables the Micro-LED transfer without any electrical or chemical forces that could damage the epitaxial layers inside the LED chip.

From the other perspective from the aforementioned transfer methods, some researchers were focused on how to easily exfoliate the Micro-LEDs from their mother wafers. Figure 4(e) shows an Al_2O_3 nanomembrane formed on the sapphire substrates via the photoresist reflow and atomic layer deposition in the stage of Micro-LED chip fabrication [29]. Part of this thin film was adhered to the sapphire substrate, while most of it was suspended. By the epitaxial growth of Micro-LEDs on this nanostructure, the vertically structured LED chips were fabricated, which were attached to mother substrates with 120 nm-thick tethers. After the eutectic bonding between the vertical Micro-LEDs and the target substrates, these LED chips were mechanically transferred by the fracture of nanomembrane bridges. This Micro-LED chip fabrication on the nanomembrane enables the Micro-LED transfer without conventional laser lift-off.

3. MICRO-LED BONDING

3.1 ACF Bonding

After the Micro-LED transfer, the Micro-LED chips should be electrically connected to backplanes or PCBs via bonding process. To bond the Micro-LEDs with target substrates, anisotropic conductive film (ACF) has been utilized. The ACF consists of epoxy resin and conductive polymer balls. Under heat and pressure, the conductive particles are mechanically deformed to form electrical contact between chips and substrates, while the epoxy resin is chemically cured to adhere the chips to the substrates. For the commercialization of Micro-LED displays, Micro-LEDs must be integrated with active-matrix backplanes consisting of Si TFTs or oxide TFTs to display colorful and high-resolution images in TVs, tablets, and smart-phones. Um et al. demonstrated the ACF bonding between the InGaN Micro-LEDs and the oxide TFT backplane for the realization of an active-matrix Micro-LED display [30]. The flip-chip structured Micro-LEDs were fabricated on the sapphire substrates, while the oxide TFTs were fabricated on the glass substrates. The ACF bonding was performed to electrically connect the Micro-LEDs with the underlying backplane, followed by laser lift-off process to remove the sapphire substrates [Fig. 5(a)]. After the Micro-LED bonding, the yield of bonding process was evaluated by applying voltage on all the 2-inch scale Micro-LED display. During the voltage increase from 2 V to 5 V, the whole Micro-LED area of the display emitted blue light. As a result, a 384 × 128 array of blue Micro-LEDs was integrated with the oxide TFTs to demonstrate the monochromatic Micro-LED display with distinctive images, as shown in [Fig. 5(b)]. This work implies that ACF bonding is applicable not only to the conventional interconnection between flexible PCBs and drivers, but also to the fabrication of active-matrix Micro-LED displays. To demonstrate full-color Micro-LED displays via ACF bonding, AlGaInP red LEDs also need to be integrated with display substrates via ACF. Figure 5(c) schematically illustrates that the AlGaInP Micro-LED chips were electrically connected to the photo-sintered Cu electrodes after the ACF bonding process [31]. The LED chip assembled on the flash-activated Cu electrode exhibited superior optical performance compared with the LED integrated with the vacuum deposited Cu electrode, although both LED chips were treated by the same ACF bonding [Fig. 5(d)]. Conventional ACF consisting of epoxy resin has critical drawbacks of low stretchability and high process temperature (> 150°C) to realize stretchable Micro-LED displays. Therefore, a stretchable ACF that has 20 μm diameter microparticles in a thermoplastic block copolymer was reported, as displayed in Fig. 5(e) [32]. While conductive particles were randomly distributed in conventional ACFs, conductive microparticles were patterned in this stretchable ACF. Therefore, the conductive particles were only placed in the region of bonding between the chips and the substrates to prevent the unintentional short-circuit issue after the bonding process [Fig. 5(f)]. After the thermocompression at 80°C, the Micro-LEDs were electrically connected to the eutectic gallium-indium (EGaIn) electrodes on the PDMS substrates via the stretchable ACF, exhibiting stable operation under applied strains of up to 70%, as displayed in Fig. 5(g). These results demonstrate that the ACF bonding facilitates the reliable interconnection of Micro-

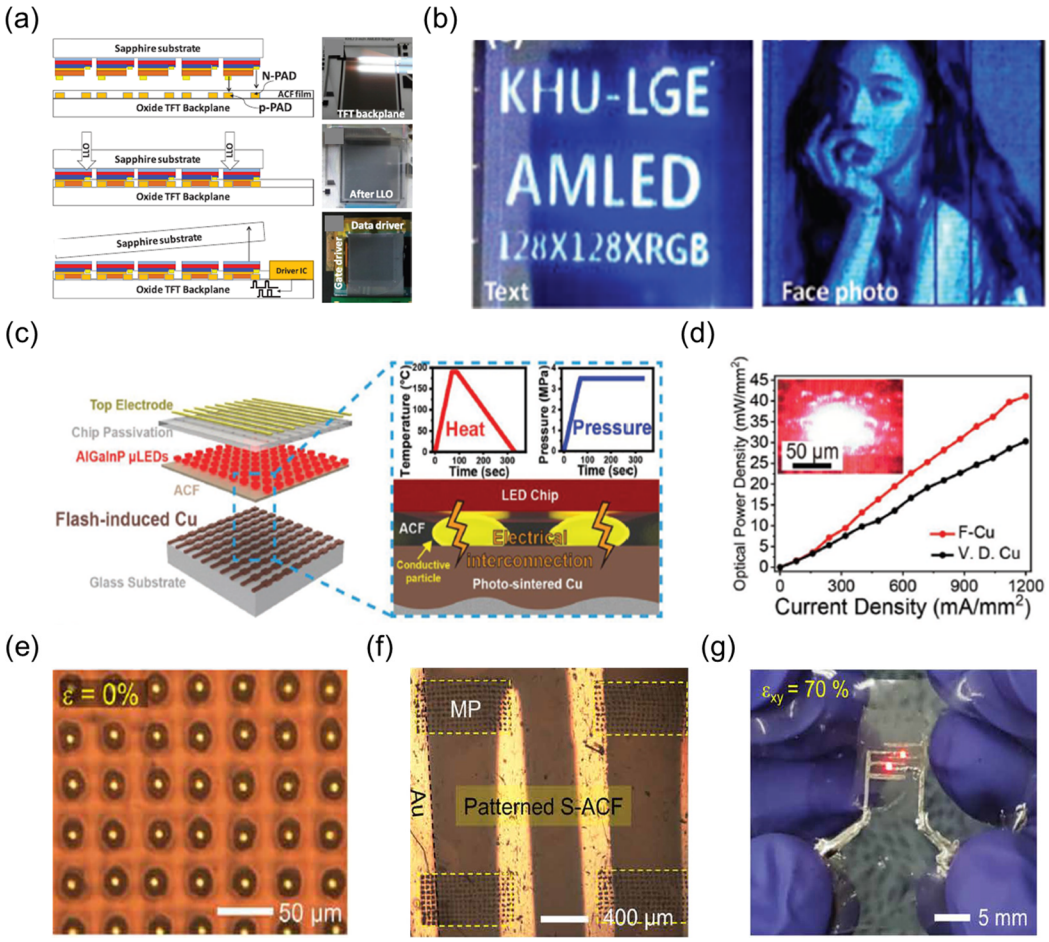

Fig. 5. (a) Schematic illustration of ACF bonding between the InGaN Micro-LEDs and the oxide thin-film transistor backplane, (b) photographs of active-matrix Micro-LED display consisting of 384 × 128 blue Micro-LEDs (Reprinted with permission from ref. [30]. Copyright 2019, Wiley-VCH), (c) schematic illustration of AlGaInP Micro-LEDs integrated with the photo-sintered Cu electrodes via ACF bonding, (d) optical power density of AlGaInP Micro-LEDs integrated with the photo-sintered Cu and the vacuum-deposited Cu electrodes via ACF bonding as a function of injection current density (Reprinted with permission from ref. [31]. Copyright 2021, Wiley-VCH), (e) top-view OM image of the stretchable ACF consisting of microparticles and a thermoplastic block copolymer, (f) top-view OM image of microparticles patterned in the stretchable ACF, and (g) photograph of Micro-LEDs integrated with EGaIn electrodes on the PDMS substrates via the stretchable ACF (Reprinted with permission from ref. [32]. Copyright 2021, AAAS).

LEDs on soft substrates as well as rigid substrates. However, conductive particles in the ACF exhibited high electrical resistance compared to solders or eutectic metals, and the film is cured after the thermocompression, which hinders Micro-LED repair.

3.2 Soldering and Eutectic Bonding

Metals have been utilized in soldering or eutectic bonding to connect the transferred Micro-LEDs to underlying target substrates [13,23,33,34]. In the field of micro-displays, conventional mass transfer of RGB Micro-LEDs has limitations in integration density and alignment accuracy, therefore, soldering has been utilized to connect CMOS backplanes with high density Micro-LEDs attached on their mother substrates. For example, Qi et al. introduced the soldering of InGaN/AlGaInP Micro-LEDs with Si COMS backplane to realize a monolithic full-color Micro-LED micro-display. Figure 6(a) shows the cross-sectional SEM image of AlGaInP and InGaN thin films, both of which were sequentially bonded with the CMOS backplane by Au-In and Au-Sn soldering, respectively [35]. To demonstrate RGB

Micro-LED display with 391 pixels per inch (ppi), red Micro-LEDs and green/blue Micro-LEDs were grown on GaAs substrates and Si substrates, respectively, followed by the sequential soldering between the Micro-LEDs and the target substrates. After each soldering process, the mother wafer was selectively removed to assemble Micro-LEDs on the backplane. Figure 6(b) shows that RGB Micro-LEDs assembled on the CMOS backplane operated stably to display a full-color image.

Eutectic bonding has also been applied to electrically connect the Micro-LEDs with display substrates. Bae et al. reported the integration of 5 μm-scale GaN Micro-LED arrays on a CMOS backplane to realize a full-color Micro-LED display, as shown in Fig. 6(d) [36]. Ni/Sn/Ti alloys were deposited on the surface of a CMOS backplane and epilayers grown on Si substrates. At a process temperature of 300°C, the epitaxial layers and the CMOS backplane were bonded by these eutectic metal alloys, followed by the removal of the Si substrates. Subsequently, the epilayers that were bonded to the CMOS backplane were mesa-etched as a form of LED chips, resulting in the integration of GaN Micro-LEDs on the CMOS backplane. Unlike soldering, the eutectic bonding is compatible to wafer bonding between the backplane and the epitaxial wafers, which facilitates the high-density integration of Micro-LEDs. Recently, Si CMOS backplanes as well as 2D-material-based high-performance backplanes have been integrated with Micro-LEDs via eutectic bonding. Li et al. reported the flip-chip eutectic bonding between InGaN Micro-LEDs and a carbon nanotube (CNT) active-matrix backplane, as described in Fig. 6(c) [37]. In bumps were formed on the CNT-based TFT array via photoresist lift-off process, and bonded with 40 μm × 40 μm sized Micro-LED at a process temperature of 200°C. Owing to the reliable interconnection between the CNT backplane and the Micro-LEDs, the CNT-

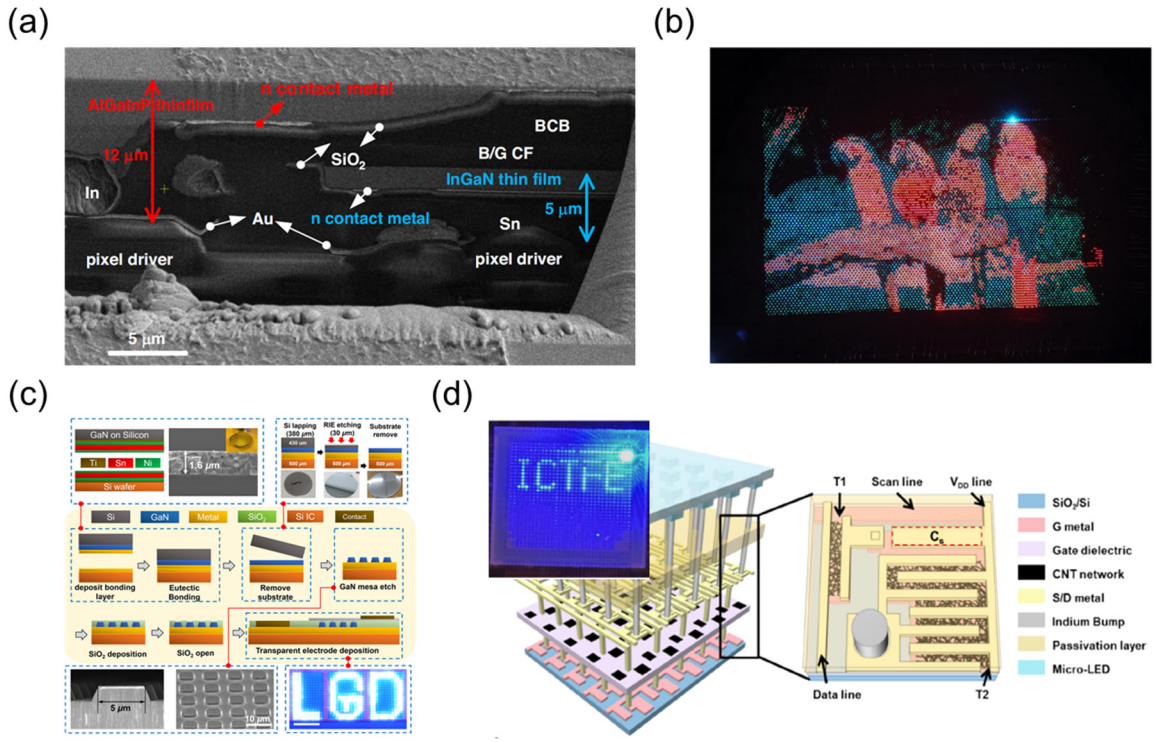

Fig. 6. (a) Cross-sectional SEM image of the AlGaInP and InGaN thin-films integrated with the CMOS backplane via the soldering, (b) photograph of 0.55-inch RGB Micro-LED display demonstrated by the sequential soldering of AlGaInP and InGaN Micro-LEDs on the CMOS backplane (Reprinted with permission from ref. [35]. Copyright 2023, Nature Publishing Group), (c) schematics of fabrication of 5 μm-scale GaN Micro-LED arrays on the CMOS backplane by utilizing wafer-level eutectic bonding (Reprinted with permission from ref. [36]. Copyright 2022, Nature Publishing Group), and (d) schematic illustration of CNT-based active-matrix Micro-LED microdisplay demonstrated by the flip-chip eutectic bonding between InGaN Micro-LEDs and CNT backplane. The inset shows a photograph of the CNT-based active-matrix Micro-LED microdisplay with 357 ppi (Reprinted with permission from ref. [37]. Copyright 2025, American Chemical Society).

based active-matrix Micro-LED micro-display (357 ppi) displayed a monochromatic image and demonstrated both pulse-amplitude-modulation and pulse-width-modulation driving [Fig. 6(d)]. The pixel yield of the Micro-LED display was close to 100%, while a single row in the display exhibited brightness degradation during the display operation. It is noteworthy that Micro-LED displays with hundreds of ppi were realized by soldering or eutectic bonding, because solders can be patterned with high resolution, down to tens of micro-meters via conventional photolithography. Furthermore, owing to low resistivity of metals, the Micro-LED devices can be utilized to display high-resolution images without RC delay.

4. NOVEL MICRO-LED DISPLAY FABRICATION METHODS

For Micro-LED display fabrication, novel techniques that are distinct from conventional Micro-LED transfer and bonding methods have been recently developed. Some researchers suggested the monolithic fabrication of Micro-LEDs on the high-electron-mobility transistors (HEMTs) [38-40]. Cai et al. introduced the direct epitaxy of Micro-LED epi-layers on top of AlGaN/GaN HEMT epi-layers [40]. The Micro-LEDs were directly fabricated on top of transistors, as shown in Fig. 7(a). PECVD oxide on an AlGaN/GaN HEMT template was dry-etched into a microhole array, followed by the HEMT layer etching with SiO_2 masks. Subsequently, InGaN Micro-LEDs were selectively grown in these holes via a metal-organic vapor-phase epitaxy. After the SiO_2 mask removal, both HEMT devices and Micro-LEDs were interconnected by the SU-8 passivation and thin-film metal lines. Unlike conventional Micro-LED fabrication processes, Micro-LEDs and transistors were integrated on the same substrates without transfer or bonding. Therefore, heterogeneous integration can be achieved without conductive media (e.g., conductive polymer balls and solders). However, this method is currently only applicable to the assembly of Micro-LEDs and HEMTs, both of which can be epitaxially grown with similar lattice structures.

Figure 7(b) shows the vertical stacking of red, green, and blue Micro-LEDs on the same substrates [41]. After the fabrication of laterally structured green Micro-LEDs on sapphire substrates, blue LED epi-wafer was bonded onto the green LEDs by the SU-8, followed by the removal of blue LED mother substrates and blue Micro-LED chip fabrication. Subsequently, red LED epi-wafer was bonded onto the blue LEDs via the same bonding method and the mother wafer removal. Red Micro-LED arrays were fabricated with the transferred red LED epi-layers. As a result, red, green, and blue Micro-LEDs were located in different layers of a pixel. Note that the epi-layers of differently colored Micro-LEDs were transferred onto the same substates, preventing the misalignment between the micro-LED chips and the substrates during the Micro-LED transfer. In order to vertically integrate red, green, and blue Micro-LEDs, 2D materials-based layer transfer also can be utilized [42]. By depositing 2D materials including as graphene and h-BN, epi-layers of Micro-LEDs were capable of being mechanically exfoliated from their mother substrates. Therefore, each epi-layer was sequentially transferred on target substrates and mesa-etched as a form of LED chip, which leads to the demonstration of full-color Micro-LEDs with 5,100 ppi. However, these vertical stacking of Micro-LEDs have a drawback of repair difficulty, because red, green, and blue Micro-LEDs were physically bonded as a one unit.

As the Micro-LED dimension decreases below 10 μm, conventional Micro-LED fabrication processes including mesa-etching and transfer have limitations of low Micro-LED performance and yield loss in realizing high-resolution Micro-LED devices for AR/VR. Li et al. reported GaN-on-GaN homoepitaxial Micro-LEDs that were based on ion-implantation [43]. F^- ion was injected in the epitaxial layers between each Micro-LED pixel [Fig. 7(c)]. This ion caused the lattice damage, and reduced the conductivity of LED epi-layers in the targeted regions. By electrically insulating the regions between Micro-LED pixels without etching process, the Micro-LEDs have no sidewalls, while conventional mesa-etched LED chips have sidewall defects that cause serious external quantum efficiency degradation. Furthermore, the LED epi-layers were grown on GaN homoepitaxial substrates to eliminate the transfer process and facilitate the LED chip miniaturization. By utilizing ion implantation and GaN homoepitaxial substrates, vertically structured blue Micro-LED was demonstrated, exhibiting stable electroluminescence and low electrical resistance compared to mesa-etched LEDs.

Choi et al. proposed a novel Micro-LED assembly technique,

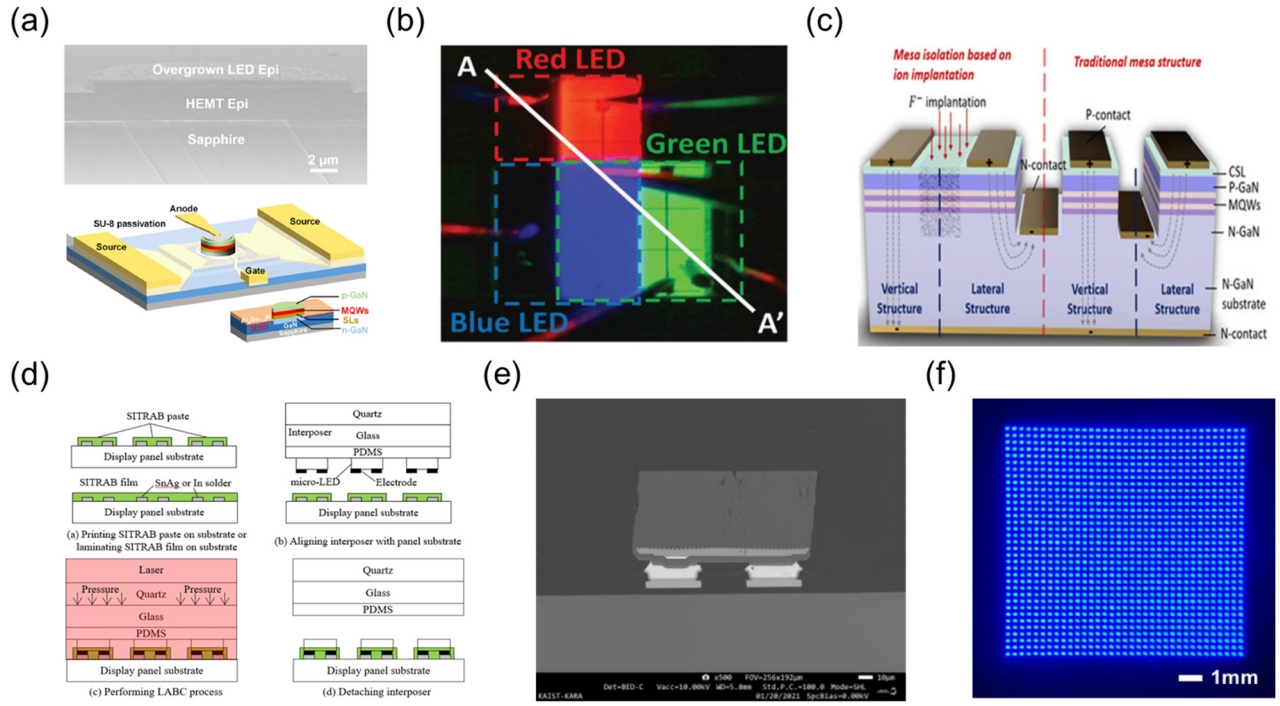

Fig. 7. (a) Cross-sectional SEM image of HEMT epi-layer and Micro-LED epi-layer, both of which were grown on the same sapphire substrates, and schematic illustration of monolithic fabrication of HEMT and Micro-LEDs (Reprinted with permission from ref. [40]. Copyright 2025, American Chemical Society), (b) OM image of vertically stacked red, green, and blue Micro-LEDs (Reprinted with permission from ref. [41]. Copyright 2021, Wiley-VCH), (c) schematic illustration of Micro-LEDs fabricated by ion implantation and mesa-etching (Reprinted with permission from ref. [43]. Copyright 2025, Wiley-VCH), (d) schematic illustration of the SITRAB method for Micro-LED assembly, (e) cross-sectional SEM image of the Micro-LED integrated with the display substrates after the SITRAB process, and (f) photograph of the Micro-LEDs assembled on the display substrates after the SITRAB process (Reprinted with permission from ref. [44]. Copyright 2021, IEEE).

called the simultaneous transfer and bonding (SITRAB) method, to transfer and bond Micro-LEDs onto display backplanes at one time [44]. Prior to the SITRAB process, the customized bonding material, called SITRAB adhesive, was coated on display substrates. This material has both functions of flux and underfill, therefore, it chemically removes surface oxide of solders during the Micro-LED assembly and physically adhere the transferred LED chips to the backplane. As described in Fig. 7(d), Micro-LEDs attached to an interposer were aligned with the bonding pads of the SITRAB adhesive-coated substrates, followed by the laser-assisted bonding with compression. Under a few seconds of infrared laser irradiation, the laser passed through the transparent interposer and generated the soldering between the metal pads of Micro-LED chips and the solder bumps of the display substrates. After the laser-induced soldering, the interposer was selectively detached, remaining the Micro-LEDs integrated with the backplane. Figure 7(e) shows the cross-sectional SEM image of the Micro-LED chip assembled on the display substrates after the SITRAB. Due to the infrared laser irradiation, the solder joints were densely formed without significant voids at the interface of the micro-scale LED chip and the underlying substrates. Therefore, the transferred Micro-LED exhibited stable operation without dead pixels, as displayed in Fig. 7(f). By the same method, a 32 × 32 resolution RGB Micro-LED display was recently demonstrated [45]. The RGB Micro-LEDs were attached to PDMS interposers with a pitch of 324 μm that corresponds to a pixel density of 8k TV display. After the SITRAB method, these Micro-LEDs were transferred and bonded onto a passive-matrix backplane consisting of Al electrodes and In solders, exhibiting a full-color image under the control of a LED driver. Furthermore, the SITRAB method enables the redundancy repair of Micro-LED displays [46]. The SITRAB-based monochromatic display exhibited the pixel yield of 98.7%, which corresponds to 13 defective pixels among 1,024

pixels. All the defective pixels were repaired by the additional SITRAB to transfer redundant Micro-LEDs onto this Micro-LED device. Unlike ACF bonding, the SITRAB utilizes the metallic solders to connect the Micro-LEDs with target substrates, facilitating the low resistive interface between the LEDs and the backplanes. Furthermore, the SITRAB adhesive generates no fume or residual flux, either of which could interfere with reliable interconnection with a pitch less than tens of micrometer. The bonding material is not cured by the SITRAB process, implying that the Micro-LED assembly can be successively performed on the same display substrates to transfer the Micro-LED arrays from different interposers. This unique capability of SITRAB method can provide powerful solutions for RGB assembly and dead-pixel repair.

5. CONCLUSION

Transfer and bonding have been critical challenges to achieve high yield in Micro-LED display manufacturing. To transfer Micro-LEDs from their mother substrates to target substrates, transfer modules or stamps generated adhesion force with the Micro-LED via Van del Waals interaction, electrostatic/electromagnetic force, and even suction. To passively align the transferred Micro-LEDs on the backplane, electric fields and temporary molds were utilized in fluidic self-assembly. To easily pick up the Micro-LEDs, the LED epi-layers were grown on the nanomebranes that were partially attached to the sapphire substrates with tethers. Micro-LEDs formed electrical connection with target substrates via ACF bonding, soldering, and eutectic bonding. The ACF bonding was compatible with soft substrates owing to their low process temperature, however, it suffers from high contact resistance and rework difficulty. Soldering and eutectic bonding generate metallic bonding between the Micro-LED chips and the underlying substrates under heat and pressure, enabling Micro-LED displays with pixel densities of several hundred ppi. Novel fabrication methods have been introduced to realize Micro-LED displays. Both Micro-LEDs and HEMT devices were monolithically fabricated on the same substates, and RGB Micro-LEDs were vertically stacked by transferring the epi-layers of Micro-LEDs. SITRAB method, which was based on the laser-assisted bonding, was implemented to transfer and bond Micro-LEDs onto target substrates in a single step.

To achieve a production yield exceeding 99.9999% in Micro-LED displays, manufacturing processes should be established by considering the characteristics of transfer and bonding methods. For instance, the SITRAB method utilizes the infrared laser to bond Micro-LEDs to display substrates. Therefore, the Micro-LEDs that are attached to highly transparent PDMS stamps or interposers in infrared wavelength can be easily integrated to display substrates without serious misalignment. We believe that improving process yield and rate in the stage of Micro-LED transfer and bonding could practically facilitate the mass-production and commercialization of Micro-LED displays.

ORCID

Jungho Shin https://orcid.org/0009-0007-0016-4530

ACKNOWLEDGEMENT

This work was supported by the Technology Innovation Programs (RS-2024-00408495, RS-2025-02308294) funded by the Ministry of Trade, Industry & Energy (MOTIE, Korea), and the National Research Foundation of Korea (NRF) funded by the Korea government (MSIT) (No. RS-2025-21452969). This work was also supported by an internal fund/grant of the Electronics and Telecommunications Research Institute (ETRI) (25YB1100).

REFERENCES

[1] H. E. Lee, J. H. Shin, J. H. Park, S. K. Hong, S. H. Park, S. H. Lee, J. H. Lee, I.-S. Kang, and K. J. Lee, *Adv. Funct. Mater.*, **29**, 1808075 (2019).
doi: https://doi.org/10.1002/adfm.201808075

[2] Y. E. Wu, C. H. Tsai, L. Y. Chen, F. C. Chen, and H. C. Kuo, *Nanomaterials*, **15**, 693 (2025).
doi: https://doi.org/10.3390/nano15090693

[3] C. C. Lin, Y. R. Wu, H. C. Kuo, M. S. Wong, S. P. DenBaars, S. Nakamura, A. Pandey, Z. Mi, P. Tian, K. Ohkawa, D. Iida, T. Wang, Y. Cai, J. Bai, Z. Yang, Y. Qian, S. T. Wu, J. Han, C. Chen, Z. Liu, B. R. Hyun, J. H. Kim, B. Jang, H. D. Kim, H. J. Lee, Y. T. Liu, Y. H. Lai, Y. L. Li, W. Meng, H. Shen, B. Liu, X. Wang, K. L. Liang, C. J. Luo, and Y. H. Fang, *J. Phys. Photonics*, **5**, 042502 (2023).

doi: https://doi.org/10.1088/2515-7647/acf972

[4] H. Wu, X. Lin, Q. Shuai, Y. Zhu, Y. Fu, X. Liao, Y. Wang, Y. Wang, C. Cheng, Y. Liu, L. Sun, X. Luo, X. Zhu, L. Wang, Z. Li, X. Wang, D. Li, and A. Pan, *Light Sci. Appl.*, **13**, 284 (2024). doi: https://doi.org/10.1038/s41377-024-01639-3

[5] T. Y. Lee, L. Y. Chen, Y. Y. Lo, S. S. Swayamprabha, A. Kumar, Y. M. Huang, S. C. Chen, H. W. Zan, F. C. Chen, R. H. Horng, and H. C. Kuo, *ACS Photonics*, **9**, 2905 (2022). doi: https://doi.org/10.1021/acsphotonics.2c00285

[6] Z. Li, J. Wang, L. Ji, J. Zhang, and Y. Liu, *Opt. Laser Technol.*, **192**, 113411 (2025). doi: https://doi.org/10.1016/j.optlastec.2025.113411

[7] W. Chang, J. Kim, M. Kim, M. W. Lee, C. H. Lim, G. Kim, S. Hwang, J. Chang, Y. H. Min, K. Jeon, S. Kim, Y. H. Choi, and J. S. Lee, *Nature*, **617**, 287 (2023). doi: https://doi.org/10.1038/s41586-023-05889-w

[8] D. Golda, S. P. Bathurst, J. A. Higginson, A. Bibl, and J. Birkmeyer, U.S. Patent 9,828,244 (2017).

[9] M. H. Wu, Y. H. Fang, and C. H. Chao, U.S. Patent 9,607,907 (2017).

[10] M. A. Meitl, Z. T. Zhu, V. Kumar, K. J. Lee, X. Feng, Y. Y. Huang, I. Adesida, R. G. Nuzzo, and J. A. Rogers, *Nat. Mater.*, **5**, 33 (2006). doi: https://doi.org/10.1038/nmat1532

[11] X. Ji, K. Wang, H. Zhou, F. Wang, L. Yin, and J. Zhang, *Appl. Phys. Lett.*, **123**, 241102 (2023). doi: https://doi.org/10.1063/5.0177351

[12] S. H. Lee, J. Kim, J. H. Shin, H. E. Lee, I. S. Kang, K. Gwak, D. S. Kim, D. Kim, and K. J. Lee, *Nano Energy*, **44**, 447 (2018). doi: https://doi.org/10.1016/j.nanoen.2017.12.011

[13] J. Hwang, H. J. Kim-Lee, S. W. Hong, J. Y. Park, D. K. Kim, D. Kim, S. Song, J. Jeong, Y. Kim, M. J. Yeom, M. C. Yu, J. Kim, Y. Park, D. C. Shin, S. Kang, J. K. Shin, Y. Kim, E. Yoon, H. Lee, G. Yoo, J. Jeong, and K. Hwang, *Nat. Electron.*, **6**, 216 (2023). doi: https://doi.org/10.1038/s41928-022-00912-w

[14] A. Carlson, A. M. Bowen, Y. Huang, R. G. Nuzzo, and J. A. Rogers, *Adv. Mater.*, **24**, 5284 (2012). doi: https://doi.org/10.1002/adma.201201386

[15] B. J. Min, Y. J. Kim, J. H. Choi, M. W. Kim, K. T. Park, D. J. Jang, J. S. Choi, and Y. S. No, *Appl. Phys. Lett.*, **121**, 241107 (2022). doi: https://doi.org/10.1063/5.0111362

[16] R. H. Kim, D. H. Kim, J. Xiao, B. H. Kim, S. I. Park, B. Panilaitis, R. Ghaffari, J. Yao, M. Li, Z. Liu, V. Malyarchuk, D. G. Kim, A. P. Le, R. G. Nuzzo, D. L. Kaplan, F. G. Omenetto, Y. Huang, Z. Kang, and J. A. Rogers, *Nat. Mater.*, **9**, 929 (2010). doi: https://doi.org/10.1038/nmat2879

[17] T. I. Kim, J. G. McCall, Y. H. Jung, X. Huang, E. R. Siuda, Y. Li, J. Song, Y. M. Song, H. A. Pao, R. H. Kim, C. Lu, S. D. Lee, I. S. Song, G. Shin, R. Al-Hasani, S. Kim, M. P. Tan, Y. Huang, F. G. Omenetto, J. A. Rogers, and M. R. Bruchas, *Science*, **340**, 211 (2013). doi: https://doi.org/10.1126/science.1232437

[18] S. I. Park, Y. Xiong, R. H. Kim, P. Elvikis, M. Meitl, D. H. Kim, J. Wu, J. Yoon, C. J. Yu, Z. Liu, Y. Huang, K. Hwang, P. Ferreira, X. Li, K. Choquette, and J. A. Rogers, *Science*, **325**, 977 (2009). doi: https://doi.org/10.1126/science.1175690

[19] C. A. Bower, B. Raymond, C. Verreen, C. Prevatte, S. Bonafede, A. Pearson, N. Rivers, B. Keller, T. Weeks, B. Trinh, E. Vick, E. Radauscher, N. Jain, M. Samarskiy, and M. A. Meitl, *IEEE J. Sel. Top. Quantum Electron.*, **29**, 2000111 (2022). doi: https://doi.org/10.1109/JSTQE.2022.3211909

[20] M. Choi, B. Jang, W. Lee, S. Lee, T. W. Kim, H. J. Lee, J. H. Kim, and J. H. Ahn, *Adv. Funct. Mater.*, **27**, 1606005 (2017). doi: https://doi.org/10.1002/adfm.201606005

[21] B. Jang, S. Won, J. Kim, J. Kim, M. Oh, H. J. Lee, and J. H. Kim, *Adv. Funct. Mater.*, **32**, 2113299 (2022). doi: https://doi.org/10.1002/adfm.202113299

[22] H. K. Park, S. W. Yoon, Y. J. Eo, W. W. Chung, G. Y. Yoo, J. H. Oh, K. N. Lee, W. Kim, and Y. R. Do, *Sci. Rep.*, **6**, 28312 (2016). doi: https://doi.org/10.1038/srep28312

[23] D. Lee, S. Cho, C. Park, K. R. Park, J. Lee, J. Nam, K. Ahn, C. Park, K. Jeon, H. Yuh, W. Choi, C. H. Lim, T. Kwon, Y. H. Min, M. Joo, Y. H. Choi, J. S. Lee, C. Kim, and S. Kwon, *Nature*, **619**, 755 (2023). doi: https://doi.org/10.1038/s41586-023-06167-5

[24] S. Lee, Y. J. Eo, M. Ko, S. Ahn, S. Yun, H. J. Kim, E. Hong, Y. Kwon, H. Kang, Y. J. Lee, G. Y. Yoo, K. N. Lee, J. K. Song, J. K. Kim, H. M. Cho, and Y. R. Do, *Nat. Commun.*, **15**, 9536 (2024). doi: https://doi.org/10.1038/s41467-024-53965-0

[25] K. Hwang, J. Hwang, Y. Kim, S. Song, K. Kong, Y. Oh, D. Chung, M. C. Yu, D. Kim, J. Y. Park, J. Moon, S. Kim, T. G. Kim, G. Lee, M. J. Yeom, J. Kim, D. C. Shin, D. K. Kim, S. W. Hong, H. J. Kim-Lee, J. Jeong, H. Lee, and G. Yoo, *Adv. Mater.*, **37**, 2416015 (2025). doi: https://doi.org/10.1002/adma.202416015

[26] Z. Liu, C. H. Lin, B. R. Hyun, C. W. Sher, Z. Lv, B. Luo, F. Jiang, T. Wu, C. H. Ho, H. C. Kuo, and J. H. He, *Light Sci. Appl.*, **9**, 83 (2020). doi: https://doi.org/10.1038/s41377-020-0268-1

[27] M. S. Kim, J. An, J. H. Lee, S. H. Lee, S. Min, Y. B. Kim, M. Song, S. H. Park, K. Y. Nam, H. J. Park, K. S. Kim, S. H. Oh, D. Hahn, J. Moon, J. W. Park, J. S. Park, T. S. Kim, B. J. Kim, and K. J. Lee, *Adv. Mater.*, **36**, 2411651 (2024). doi: https://doi.org/10.1002/adma.202411651

[28] S. H. Park, T. J. Kim, H. E. Lee, B. S. Ma, M. Song, M. S. Kim, J. H. Shin, S. H. Lee, J. H. Lee, Y. B. Kim, K. Y. Nam, H. J. Park, T. S. Kim, and K. J. Lee, *Nat. Commun.*, **14**, 7744 (2023).

doi: https://doi.org/10.1038/s41467-023-43342-8

[29] S. Park, J. E. Ryu, T. H. Kim, H. J. Kim, J. Bu, S. J. Seo, J. H. Baek, Y. J. Hong, S. W. Ryu, Y. Park, M. G. Lee, and H. W. Jang, *ACS Appl. Mater. Interfaces*, **16**, 42426 (2024).
doi: https://doi.org/10.1021/acsami.4c05958

[30] J. G. Um, D. Y. Jeong, Y. Jung, J. K. Moon, Y. H. Jung, S. Kim, S. H. Kim, J. S. Lee, and J. Jang, *Adv. Electron. Mater.*, **5**, 1800617 (2019).
doi: https://doi.org/10.1002/aelm.201800617

[31] J. H. Shin, J. H. Park, J. Seo, T. H. Im, J. C. Kim, H. E. Lee, D. H. Kim, K. Y. Woo, H. Y. Jeong, Y. H. Cho, T. S. Kim, I. S. Kang, and K. J. Lee, *Adv. Mater.*, **33**, 2007186 (2021).
doi: https://doi.org/10.1002/adma.202007186

[32] H. Hwang, M. Kong, K. Kim, D. Park, S. Lee, S. Park, H. J. Song, and U. Jeong, *Sci. Adv.*, **7**, eabh0171 (2021).
doi: https://doi.org/10.1126/sciadv.abh0171

[33] X. Zhang, P. Li, X. Zou, J. Jiang, S. H. Yuen, C. W. Tang, and K. M. Lau, *IEEE Photonics Technol. Lett.*, **31**, 865 (2019).
doi: https://doi.org/10.1109/LPT.2019.2910729

[34] W. C. Chong, W. K. Cho, Z. J. Liu, C. H. Wang, and K. M. Lau, *Proc. IEEE Compound Semicond. Integr. Circuit Symp. (CSICS)* (IEEE, La Jolla, CA, USA, 2014), p. 1.
doi: https://doi.org/10.1109/CSICS.2014.6978524

[35] L. Qi, P. Li, X. Zhang, K. M. Wong, and K. M. Lau, *Light Sci. Appl.*, **12**, 258 (2023).
doi: https://doi.org/10.1038/s41377-023-01298-w

[36] J. Bae, Y. Shin, H. Yoo, Y. Choi, J. Lim, D. Jeon, I. Kim, M. Han, and S. Lee, *Nat. Commun.*, **13**, 1862 (2022).
doi: https://doi.org/10.1038/s41467-022-29538-4

[37] Y. Li, Y. Guo, J. Li, M. Xi, L. Bai, J. Zhang, S. Li, X. Zhu, Y. He, B. He, X. Chen, Y. Zhang, Y. Gong, Z. Yin, J. Kang, L. M. Peng, R. Zhang, Y. Zhou, Y. Cao, and X. Liang, *ACS Nano*, **19**, 22837 (2025).
doi: https://doi.org/10.1021/acsnano.5c00672

[38] C. Liu, Y. Cai, X. Zou, and K. M. Lau, *IEEE Photonics Technol. Lett.*, **28**, 1130 (2016).
doi: https://doi.org/10.1109/LPT.2016.2532338

[39] Y. J. Lee, Z. P. Yang, P. G. Chen, Y. A. Hsieh, Y. C. Yao, M. H. Liao, M. H. Lee, M. T. Wang, and J. M. Hwang, *Opt. Express*, **22**, A1589 (2014).
doi: https://doi.org/10.1364/OE.22.0A1589

[40] Y. Cai, J. I. H. Haggar, C. Zhu, P. Feng, J. Bai, and T. Wang, *ACS Appl. Electron. Mater.*, **3**, 445 (2021).
doi: https://doi.org/10.1021/acsaelm.0c00985

[41] S. H. Mun, C. M. Kang, J. H. Min, S. Y. Choi, W. L. Jeong, G. G. Kim, J. S. Lee, K. P. Kim, H. C. Ko, and D. S. Lee, *Adv. Mater. Interfaces*, **8**, 2100300 (2021).
doi: https://doi.org/10.1002/admi.202100300

[42] J. Shin, H. Kim, S. Sundaram, J. Jeong, B. I. Park, C. S. Chang, J. Choi, T. Kim, M. Saravanapavanantham, K. Lu, S. Kim, J. M. Suh, K. S. Kim, M. K. Song, Y. Liu, K. Qiao, J. H. Kim, Y. Kim, J. H. Kang, J. Kim, D. Lee, J. Lee, J. S. Kim, H. E. Lee, H. Yeon, H. S. Kum, S. H. Bae, V. Bulovic, K. J. Yu, K. Lee, K. Chung, Y. J. Hong, A. Ougazzaden, and J. Kim, *Nature*, **614**, 81 (2023).
doi: https://doi.org/10.1038/s41586-022-05612-1

[43] Z. Li, Y. Liu, H. Jiang, F. Feng, J. Zhang, S. Huang, F. Yeung, M. Tseng, M. Wong, H. S. Kwok, and Z. Liu, *Adv. Sci.*, e06784 (2025).
doi: https://doi.org/10.1002/advs.202506784

[44] K. S. Choi, J. Joo, Y. S. Eom, G. M. Choi, K. S. Jang, C. Lee, S. H. Moon, H. G. Yun, J. H. Choi, and J. W. Choi, *Proc. IEEE Electron. Components Technol. Conf. (ECTC)* (IEEE, 2021), p. 1607.
doi: https://doi.org/10.1109/ECTC32696.2021.00255

[45] J. Joo, G. M. Choi, J. Shin, C. Lee, Y. S. Eom, K. S. Jang, J. H. Oh, J. E. Jung, G. E. Lee, and K. S. Choi, *SID Symp. Dig. Tech. Pap.*, **55**, 1309 (2024).
doi: https://doi.org/10.1002/sdtp.17785

[46] J. Shin, J. Joo, G. M. Choi, C. Lee, Y. H. Moon, K. S. Jang, J. H. Oh, J. E. Jung, G. E. Lee, Y. S. Eom, and K. S. Choi, *SID Symp. Dig. Tech. Pap.*, **55**, 1278 (2024).
doi: https://doi.org/10.1002/sdtp.17777